



Solvent-Induced Crystallization Method for High-Performance and Long-Term Stability Flexible Perovskite Photodetectors

Zhang Lei¹, Li Shugang², Zhang Tianjun², Song Shuang² and Pan Hongyu^{2*}

¹College of Energy Engineering, Xi'an University of Science and Technology, Xi'an, China, ²School of Safety Science and Engineering, Xi'an University of Science and Technology, Xi'an, China

Herein, we report a novel solvent-induced fabrication method to synthesize a perovskite thin film on flexible substrates. The high-quality CH₃NH₃PbI₃ (MAPbI₃) thin film is successfully fabricated, which is applied to prepare the stable flexible photodetector (PD). Compared with the reported results, this method achieved a low-temperature and low-cost perovskite thin film fabrication process on a flexible substrate. The constructed MAPbI₃ layer possesses the advantages of being highly crystalline, uniform, and compact in a large area. The flexible PD based on the as-prepared perovskite thin film exhibits excellent performance and long-term stability. The EQE and R of the flexible PDs reached 8 × 10²% and 3.6 A/W, respectively. At the same time, the flexible PDs still showed superior stability and high performance after 15 days of continuous working. The presented high-quality perovskite thin-film fabrication method and high-performance flexible perovskite PDs are expected for application in the development of novel optoelectronic devices.

Keywords: flexible photodetector, organometal halide perovskite, solvent-induced crystallization, photodetector, hybrid perovskite

OPEN ACCESS

Edited by:

Jun Xi,
Xi'an Jiaotong University, China

Reviewed by:

Xiaobao Xu,
Nanjing University of Science and
Technology, China

Maning Liu,
Tampere University, Finland

*Correspondence:

Pan Hongyu
pan05016@126.com

Specialty section:

This article was submitted to
Semiconducting Materials and
Devices,
a section of the journal
Frontiers in Materials

Received: 24 March 2022

Accepted: 23 May 2022

Published: 22 July 2022

Citation:

Lei Z, Shugang L, Tianjun Z, Shuang S
and Hongyu P (2022) Solvent-Induced
Crystallization Method for High-
Performance and Long-Term Stability
Flexible Perovskite Photodetectors.
Front. Mater. 9:903308.
doi: 10.3389/fmats.2022.903308

1 INTRODUCTION

Opto-electronic devices constructed on flexible substrates are emerging in different areas, including industry, military, and research. Their applications, such as portable display, sensor, detector, and solar cell, have been extensively explored. The advantages of high mechanical, flexibility, lightweight, and low manufactured temperature are preferable for advanced portable and wearable electronic equipment (Hamers, 2001; Park et al., 2012; Zheng et al., 2017). A photodetector (PD) is an important opto-electronic device for detecting optical signals and converting them into electrical ones (Sze et al., 1971; Dou et al., 2014; Alwadai et al., 2017; Bai et al., 2018). For decades, flexible PDs have attracted considerable attention owing to their enormous commercial applications. Unfortunately, the poor device performance and high working voltage remain to be figured out in order to realize their practical application in low-cost and flexible opto-electronic systems (Park et al., 2012).

Recently, a new group of organic-inorganic halide perovskite (OIHP) materials are demonstrated to be a class of excellent semiconductors. The OIHPs own outstanding optical and electronic performance characteristics, such as direct bandgap, high light absorption coefficient, and excellent charge carrier transport properties (Kojima et al., 2009; Lee et al., 2012; Yamada et al., 2014; Zhou et al., 2014; Li et al., 2019). Obviously, the OIHP-based photovoltaic cells show advanced rapid power conversion efficiency

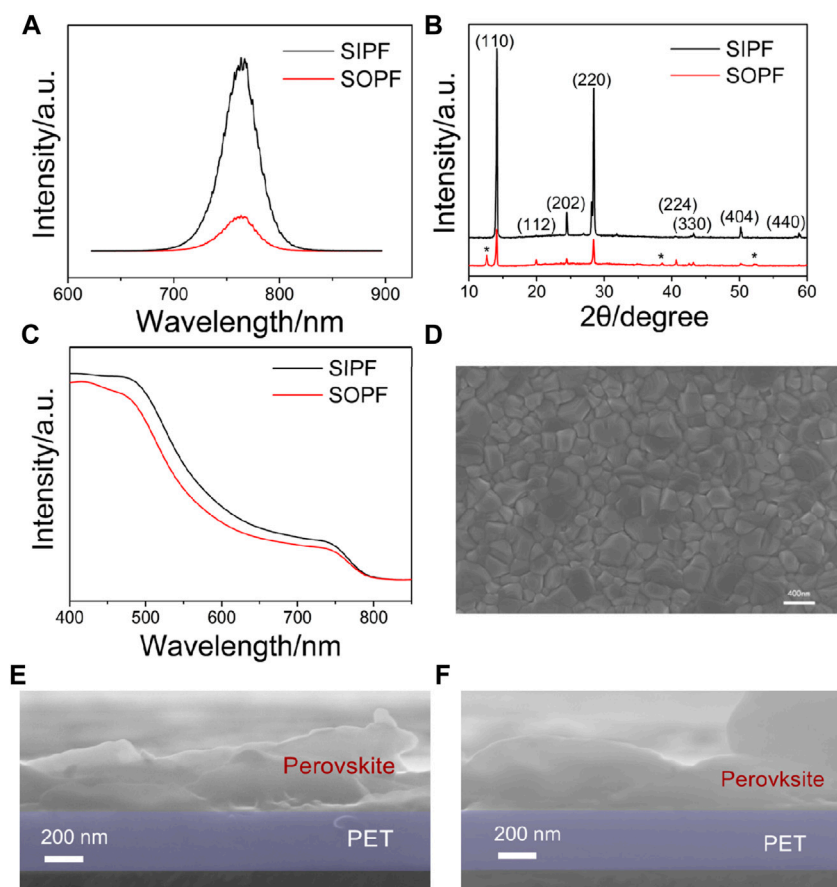


FIGURE 1 | Characterization of the constructed perovskite thin film based on the solvent-induced method. **(A)** time-resolved PL, **(B)** XRD, and **(C)** absorption spectrum. **(D)** top-view SEM image of the SIPF **(E)** and **(F)** cross-section SEM images for the SOPF and SIPF films.

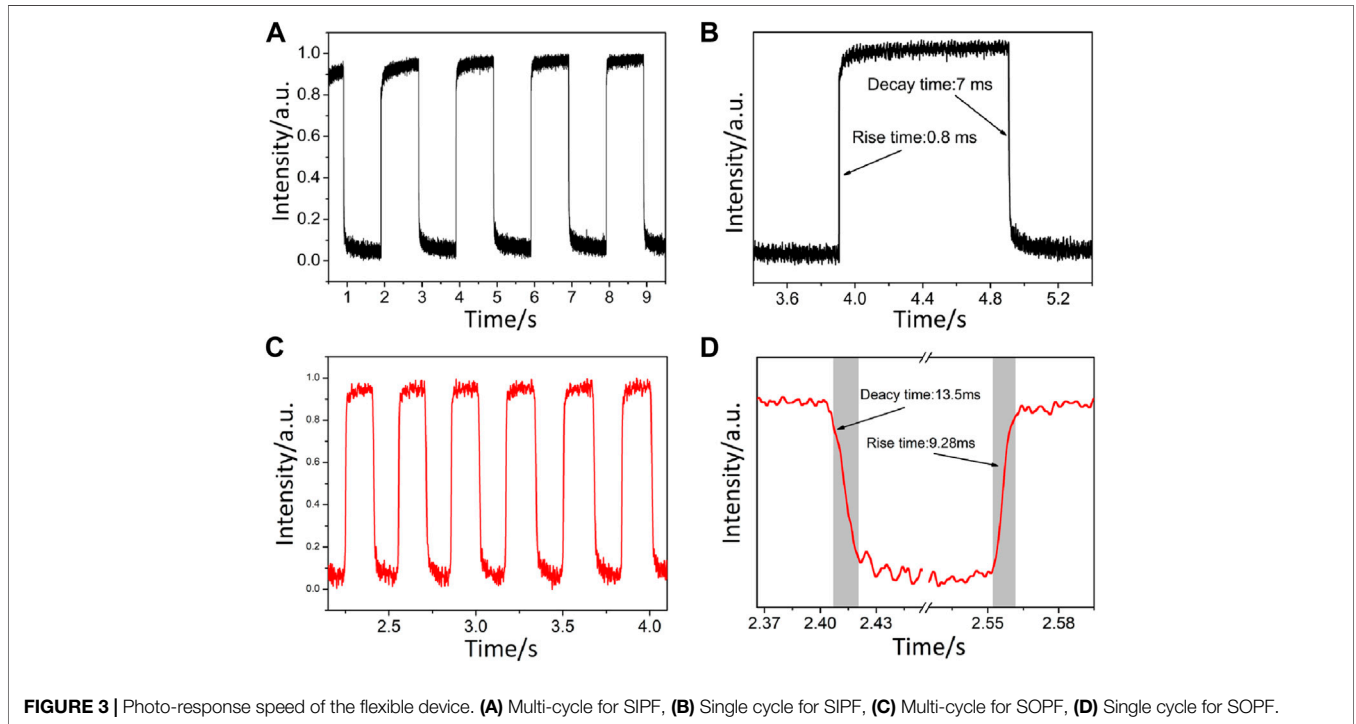
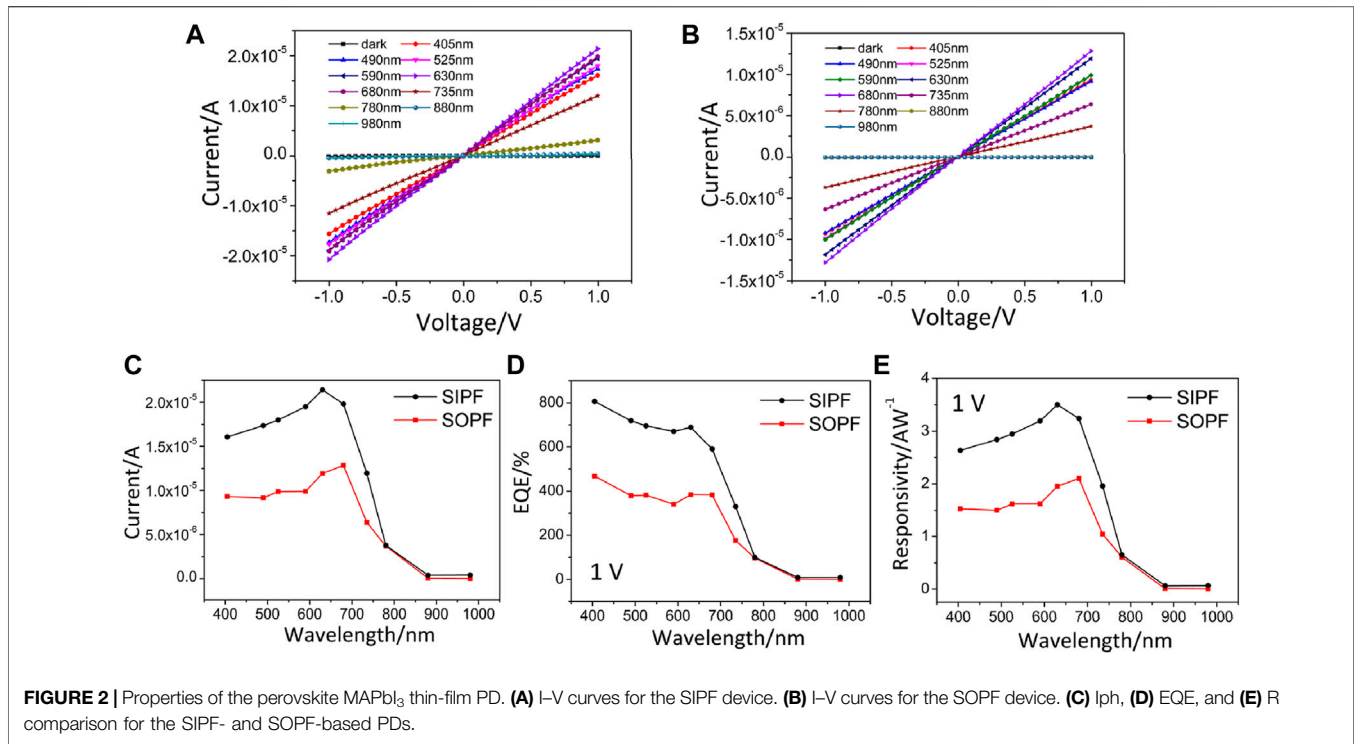
and reach the highest value of over 25% so far (Dong et al., 2015; Saidaminov et al., 2016; Lin et al., 2017). The perovskite materials have also been investigated in other opto-electronic devices of light-emitting diodes, lasers, and PDs (Caldeira Filho and Mulato, 2011; Xia et al., 2014; Lian, 2015; Kang, 2016; Manser et al., 2016; Wang et al., 2016; Hu et al., 2017; Hu et al., 2019; Mujahid et al., 2020; Shao and Hu, 2020; Mei et al., 2021).

Based on the reported results so far, the flexible perovskite devices have relatively lower performance than the devices on rigid wafers. One of the key shortcomings is that a compact and large-area high-quality perovskite active layer cannot be effectively constructed on flexible substrates. In order to obtain a high-quality material, herein, solvent engineering is introduced in this work. The manufacturing process is performed on a bendable poly(ethylene terephthalate) (PET) substrate. The perovskite thin film, achieved by the novel solvent-induced method, shows combination properties, namely, highly compact and crystalline. Using the as-grown perovskite film, a metal–semiconductor–metal PD has also been successfully constructed. The resulting PD exhibits enhanced performance of higher performance and lower working voltage which achieves a maximum external quantum efficiency (EQE) of $8 \times 10^2\%$ and a responsivity (R) of 3.7 A/W at a low bias of 1 V, respectively. The

method shows a potential approach in the fabrication of a high-quality perovskite layer on a flexible substrate. The flexible perovskite PD demonstrates great potential applications in low-cost photo-detection and high-resolution imaging areas.

2 EXPERIMENT, RESULTS, AND DISCUSSION

The PET substrate covered with the ITO electrode is first patterned by a photolithography technique. The ITO interdigital electrodes are formed with a space length of 0.02 mm, and the active area of the device is defined by about 1 mm². The OIHP $\text{CH}_3\text{NH}_3\text{PbI}_3$ (MAPbI₃) precursor solution is made of methylammonium iodide ($\text{CH}_3\text{NH}_3\text{I}$) and lead iodide (PbI_2) with a molar ratio of 1:1 being dissolved in anhydrous *N,N*-dimethylformamide (DMF) (concentrations of 650 mg ml⁻¹). Then, the solution is vigorously stirred for about 12 h at 60°C. The perovskite thin film is constructed on a patterned ITO/PET substrate by a solvent-induced technology. First, a DMF solution of the perovskite precursor is spin-coated on the flexible wafer. After a 6 s delay, a small amount of chlorobenzene is added to the wet film in order to induce crystallization, and the formed sample is annealed at 100°C for 30 min on a hot plate. A dense



perovskite film is synthesized, and a PD has also been constructed on the ITO/PET substrate. The active layer is characterized first below, and the solvent-induced perovskite film (SIPF) has also been compared with that of the spin-coated only perovskite film

(SOPF). **Figure 1A** is the steady-state photoluminescence (PL) spectrum of the perovskite layers. The peak wavelength is located at 765 nm, and the intensity of the SIPF is much higher than that of an SOPF. The X-ray diffraction (XRD) pattern, as shown in **Figure 1B**,

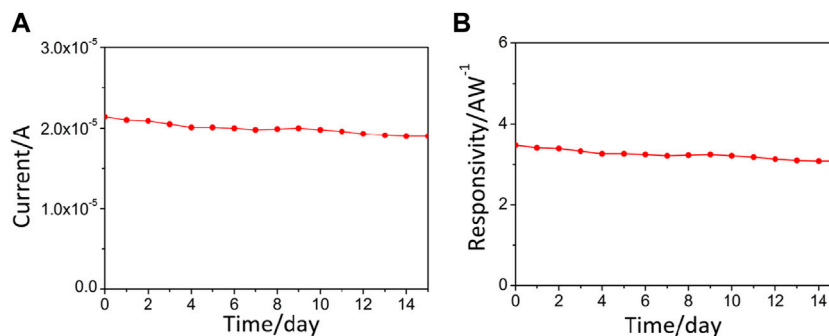


FIGURE 4 | Long-term stability of the SIFP-based PD. **(A)** photocurrent and **(B)** responsivity changing with time.

exhibits a preferential growth at the (110) crystal face with a tetragonal structure, indicating that SIFP shows higher crystallinity than the SOPF. As shown in **Figure 1C**, the absorption spectra of the perovskite thin film are characterized by an ultraviolet-visible spectrophotometer machine. It indicates that the active layer absorbs the photon's energy higher than 800 nm. The absorption ability of the SIFP is higher than that of an SOPF. The morphology of the solvent-induced perovskite film is investigated by scanning electron microscopy (SEM) as shown in **Figure 1D**, which exhibits a composed and pinhole-free surface with fine crystalline nature. The cross-sectional SEM images for the SOPF and SIFP are presented in **Figures 1E and F**, respectively. It also proves that the SIFP shows compact and uniform properties. However, there are many pinholes in the SOPF which is similar to those in the reported works.

Current-voltage (I - V) curves of the flexible PD are analyzed by a digital source meter Keithley 2,400 in the atmosphere at room temperature. A set of light-emitting diodes with different wavelengths are used for the incident light source. As shown in **Figure 2A**, the SIFP-based device dark current (I_{dark}) and photocurrents under illumination light changing from 405 to 880 nm are exhibited. The I_{dark} obtained from the data, is 4×10^{-7} A at 1 V bias. When the PD is illuminated, the photocurrents (I_{ph}) are defined as the current difference between illumination and dark which increased dramatically and peaked under the wavelength of 630 nm. The highest I_{ph} value is 2×10^{-5} A, which is two orders higher than the I_{dark} . **Figure 2B** shows the I - V curves for the SOPF-based PD. Its highest I_{ph} is about half of the SIFP-based device. The photo-to-dark current ratio (I_{ph}/I_{dark}), which is a very important parameter for a PD, becomes doubly higher based on the obtained data. It indicates the high-quality perovskite film-based flexible PD has an enhanced signal-to-noise ratio. The I_{ph} comparison results for the two devices are presented in **Figure 2C** in detail. To further evaluate the performance of the flexible PDs, the critical parameters, EQE and R , are obtained and discussed in detail below. $EQE = I_{ph}/q\Phi$, defined as the number of carriers produced per photon, and $R = I_{ph}/P_{in}$, defined as the ratio of photocurrent to incident light intensity, in which q is the elementary charge, Φ is the photon flux, and P_{in} is the incident optical power. The EQE and R of the PDs are shown in **Figures 2D and E**. At a bias of 1 V, the SIFP-based PD owns the highest EQE of 805% and the highest R -value of 3.6 A/W at the wavelength of 630 nm. The device on-off switch speed experiments are then performed. **Figure 3** shows time-resolved

on-off switching behaviors of the PD investigated at a wavelength of 630 nm. The rising and decay time of the flexible PD is measured to be 0.8 and 7 ms at room temperature, respectively, which are comparable with the rigid-wafer-based devices. These results indicate that the novel strategy of an anti-solvent induced crystal can also be used in the fabrication of the perovskite layer on the plastic substrates. It can be used for the construction of a high-quality perovskite film and high-performance opto-electronic devices.

Stability is an important factor affecting device suitability for practical applications in portable electronic devices. The long-term stability tests are then performed while being encapsulated by a PMMA film. **Figures 4A and B** show the device performance changing with the working time. The SIFP-based flexible PD shows a high stable I_{ph} , EQE , and R after working, lasting over 15 days. This suggests that the obtained high-quality perovskite film is characterized by excellent long-term stability.

3 CONCLUSION

In summary, a novel solvent-induced fabrication method has been used to synthesize perovskite thin films on flexible substrates. The high-quality MAPbI₃ thin film is successfully fabricated and further applied to the flexible PD. Compared with the reported results, this method achieves a low-temperature and low-cost perovskite thin film fabrication process on a flexible substrate. The constructed MAPbI₃ layer possesses the advantages of being highly crystalline, uniform, and compact in a large area. The flexible PD based on the as-prepared perovskite thin film exhibits excellent performance and long-term stability. The EQE and R of the flexible PDs reached $8 \times 10^2\%$ and 3.6 A/W, respectively. At the same time, the flexible PDs still showed superior stability and high performance after 15 days of continuous working. The presented high-quality perovskite thin-film fabrication method and high-performance flexible perovskite PDs are expected to be applied in developing novel opto-electronic devices.

DATA AVAILABILITY STATEMENT

The raw data supporting the conclusions of this article will be made available by the authors, without undue reservation.

AUTHOR CONTRIBUTIONS

ZL and SS performed the experiments and measurements. PH supervised this work. TZ and SL reviewed and edited this manuscript.

REFERENCES

- Alwadai, N., Haque, M. A., Mitra, S., Flemban, T., Pak, Y., Wu, T., et al. (2017). High-Performance Ultraviolet-To-Infrared Broadband Perovskite Photodetectors Achieved via Inter-/Intraband Transitions. *ACS Appl. Mat. Interfaces* 9, 37832–37838. doi:10.1021/acsami.7b09705
- Bai, F., Qi, J., Li, F., Fang, Y., Han, W., Wu, H., et al. (2018). A High-Performance Self-Powered Photodetector Based on Monolayer MoS₂/Perovskite Heterostructures. *Adv. Mat. Interfaces* 5, 1701275. doi:10.1002/admi.201701275
- Caldeira Filho, A. M., and Mulato, M. (2011). Characterization of Thermally Evaporated Lead Iodide Films Aimed for the Detection of X-Rays. *Nucl. Instrum. Methods Phys. Res. Sect. A Accel. Spectrom. Detect. Assoc. Equip.* 636, 82–86. doi:10.1016/j.nima.2011.01.093
- Dong, R., Fang, Y., Chae, J., Dai, J., Xiao, Z., Dong, Q., et al. (2015). High-Gain and Low-Driving-Voltage Photodetectors Based on Organolead Triiodide Perovskites. *Adv. Mat.* 27, 1912–1918. doi:10.1002/adma.201405116
- Dou, L., Yang, Y., You, J., Hong, Z., Chang, W.-H., Li, G., et al. (2014). Solution-processed Hybrid Perovskite Photodetectors with High Detectivity. *Nat. Commun.* 5, 5404. doi:10.1038/ncomms6404
- Hamers, R. J. (2001). Flexible Electronic Futures. *Nature* 412, 489–490. doi:10.1038/35087682
- Hu, W., Cong, H., Huang, W., Huang, Y., Chen, L., Pan, A., et al. (2019). Germanium/Perovskite Heterostructure for High-Performance and Broadband Photodetector from Visible to Infrared Telecommunication Band. *Light Sci. Appl.* 8, 106. doi:10.1038/s41377-019-0218-y
- Hu, W., Huang, W., Yang, S., Wang, X., Jiang, Z., Zhu, X., et al. (2017). High-Performance Flexible Photodetectors Based on High-Quality Perovskite Thin Films by a Vapor-Solution Method. *Adv. Mat.* 29, 1703256. doi:10.1002/adma.201703256
- Kang, D. H. (2016). An Ultrahigh-Performance Photodetector Based on a Perovskite-Transition-Metal-Dichalcogenide Hybrid Structure. *Adv. Mat.* 28, 7799. doi:10.1002/adma.201600992
- Kojima, A., Teshima, K., Shirai, Y., and Miyasaka, T. (2009). Organometal Halide Perovskites as Visible-Light Sensitizers for Photovoltaic Cells. *J. Am. Chem. Soc.* 131, 6050–6051. doi:10.1021/ja809598r
- Lee, M. M., Teuscher, J., Miyasaka, T., Murakami, T. N., and Snaith, H. J. (2012). Efficient Hybrid Solar Cells Based on Meso-Superstructured Organometal Halide Perovskites. *Science* 338, 643–647. doi:10.1126/science.1228604
- Li, N., Tao, S., Chen, Y., Niu, X., Onwudinanti, C. K., Hu, C., et al. (2019). Cation and Anion Immobilization through Chemical Bonding Enhancement with Fluorides for Stable Halide Perovskite Solar Cells. *Nat. Energy* 4, 408–415. doi:10.1038/s41560-019-0382-6
- Lian, Z. (2015). High-Performance Planar-Type Photodetector on (100) Facet of MAPbI₃ Single Crystal. *Sci. Rep.* 5, 16563. doi:10.1038/srep07723
- Lin, Y. H., Pattanasattayavong, P., and Anthopoulos, T. D. (2017). Metal-Halide Perovskite Transistors for Printed Electronics: Challenges and Opportunities. *Adv. Mat.* 29, 1702838. doi:10.1002/adma.201702838
- Manser, J. S., Saidaminov, M. I., Christians, J. A., Bakr, O. M., and Kamat, P. V. (2016). Making and Breaking of Lead Halide Perovskites. *Acc. Chem. Res.* 49, 330–338. doi:10.1021/acs.accounts.5b00455
- Mei, J., Liu, M., Vivo, P., and Pecunia, V. (2021). Two-Dimensional Antimony-Based Perovskite-Inspired Materials for High-Performance Self-Powered Photodetectors. *Adv. Funct. Mat.* 31, 2106295. doi:10.1002/adfm.202106295
- Mujahid, M., Chen, C., Hu, W., Wang, Z.-K., and Duan, Y. (2020). Progress of High-Throughput and Low-Cost Flexible Perovskite Solar Cells. *Sol. RRL* 4, 1900556. doi:10.1002/solr.201900556
- Park, S., Wang, G., Cho, B., Kim, Y., Song, S., Ji, Y., et al. (2012). Flexible Molecular-Scale Electronic Devices. *Nat. Nanotech* 7, 438–442. doi:10.1038/nnano.2012.81
- Saidaminov, M. I., Haque, M. A., Savoie, M., Abdelhady, A. L., Cho, N., Dursun, I., et al. (2016). Perovskite Photodetectors Operating in Both Narrowband and Broadband Regimes. *Adv. Mat.* 28, 8144–8149. doi:10.1002/adma.201601235
- Shao, C.-R., and Hu, W. (2020). Lateral Epitaxial Grown of Two-Dimensional Halide Perovskite Heterostructures. *Rare Met.* 39 (8), 863–864. doi:10.1007/s12598-020-01458-6
- Sze, S. M., Coleman, D. J., and Loya, A. (1971). Current Transport in Metal-Semiconductor-Metal (MSM) Structures. *Solid-State Electron.* 14, 1209–1218. doi:10.1016/0038-1101(71)90109-2
- Wang, F., Mei, J., Wang, Y., Zhang, L., Zhao, H., and Zhao, D. (2016). Fast Photoconductive Responses in Organometal Halide Perovskite Photodetectors. *ACS Appl. Mat. Interfaces* 8, 2840–2846. doi:10.1021/acsami.5b11621
- Xia, H.-R., Li, J., Sun, W.-T., and Peng, L.-M. (2014). Organohalide Lead Perovskite Based Photodetectors with Much Enhanced Performance. *Chem. Commun.* 50, 13695–13697. doi:10.1039/c4cc05960c
- Yamada, Y., Nakamura, T., Endo, M., Wakamiya, A., and Kanemitsu, Y. (2014). Photocarrier Recombination Dynamics in Perovskite CH₃NH₃PbI₃ for Solar Cell Applications. *J. Am. Chem. Soc.* 136, 11610–11613. doi:10.1021/ja506624n
- Zheng, Z., Gan, L., Zhang, J., Zhuge, F., and Zhai, T. (2017). An Enhanced UV-Vis-NIR an D Flexible Photodetector Based on Electrospun ZnO Nanowire Array/PbS Quantum Dots Film Heterostructure. *Adv. Sci.* 4, 1600316. doi:10.1002/adv.201600316
- Zhou, H., Chen, Q., Li, G., Luo, S., Song, T.-b., Duan, H.-S., et al. (2014). Interface Engineering of Highly Efficient Perovskite Solar Cells. *Science* 345, 542–546. doi:10.1126/science.1254050

FUNDING

The authors are grateful to the National Natural Science Foundation of China (51874234, 52104215, 52104216, 51774234, and 51734007).

Conflict of Interest: The authors declare that the research was conducted in the absence of any commercial or financial relationships that could be construed as a potential conflict of interest.

Publisher's Note: All claims expressed in this article are solely those of the authors and do not necessarily represent those of their affiliated organizations, or those of the publisher, the editors, and the reviewers. Any product that may be evaluated in this article, or claim that may be made by its manufacturer, is not guaranteed or endorsed by the publisher.

Copyright © 2022 Lei, Shugang, Tianjun, Shuang and Hongyu. This is an open-access article distributed under the terms of the Creative Commons Attribution License (CC BY). The use, distribution or reproduction in other forums is permitted, provided the original author(s) and the copyright owner(s) are credited and that the original publication in this journal is cited, in accordance with accepted academic practice. No use, distribution or reproduction is permitted which does not comply with these terms.